Discover Chemistry

Research

Evaluation of the physical properties of local wheat husk ash and its effects on the compressive strength of hardened cement paste

Masuoda Farhat[1] · Mohammed A. Al Madani[1] · Taha Abdullah[1] · Mohammed Embaya[2] · Abdulla Saeed[2] · Abdulla Saleh[2] · Fares Fenniche[3,4] · Yasmina Khane[4,5]

Received: 1 December 2024 / Accepted: 9 April 2025
Published online: 23 April 2025
© The Author(s) 2025 OPEN

Abstract
The dehusking of wheat results in the significant annual production of wheat husk, an agricultural byproduct. This waste is often burned outdoors to generate energy, with the resulting ash (wheat husk ash, WHA) typically disposed of in landfills, leading to environmental harm. To mitigate the negative environmental impact, this research explores the potential of utilizing wheat husk ash to enhance the mechanical properties of cement paste. The study involved the partial replacement of Portland cement in the mixture with varying proportions of wheat husk ash (0, 5, 10, 15, 20, 25 and 30%) to produce WHA blended cement with sample with 0% as the control, and examined the compressive strength of hardened cement paste (HCP) at different curing ages (3, 7, 14, and 28 days). Chemical water tests revealed that the water-to-cement ratio required for standard HCP increased linearly with the proportion of WHA in the mix. Additionally, it was found that the bulk density of HCP decreased as the percentage of WHA increased. Compressive strength tests of the HCP samples yielded promising results, particularly with 15% (30.04) and 20% (28.73) WHA replacement. The compressive strength improved by approximately 14% with 15% WHA replacement and by 10% with 20% WHA replacement. In conclusion, the incorporation of wheat husk ash (WHA) at optimal percentages in cement mixtures enhances the compressive strength of hardened cement paste, particularly after full curing. This study highlights not only the mechanical improvements achieved through WHA integration but also its potential to significantly reduce the carbon footprint of cement production, demonstrating a dual advantage of improved material performance and environmental sustainability.

Keywords Wheat husk · Wheat husk ash (WHA) · Hardened cement paste (HCP) · Compressive strength · Portland cement replacement

1 Introduction

The growing demand for sustainable construction materials is driven by the dual challenges of environmental degradation and the need for resilient infrastructure. Cement production alone is responsible for approximately 8% of global carbon dioxide emissions, making it a significant contributor to climate change. Furthermore, the generation of agricultural

✉ Yasmina Khane, yasminekhane@yahoo.fr | [1]Materials and Corrosion Engineering Department, Sebha University, Sabhā, Libya. [2]Chemical Engineering Department, Sebha University, Sabhā, Libya. [3]Process Engineering Department, Faculty of Science and Technology, Ghardaïa University, Bounoura, Algeria. [4]Materials, Energy Systems Technology and Environment Laboratory, Faculty of Sciences and Technology, University of Ghardaïa, BP 455, 47000 Ghardaïa, Algeria. [5]Faculty of Sciences and Technology, University of Ghardaïa, BP 455, 47000 Ghardaïa, Algeria.

waste, including wheat husk, poses an additional environmental burden due to its limited reuse and improper disposal practices. Innovative solutions that address both issues simultaneously are increasingly critical. One such approach is the utilization of agricultural byproducts, like wheat husk ash (WHA), as supplementary cementitious materials (SCMs) in cement and concrete production. WHA, rich in amorphous silica, has the potential to reduce the environmental footprint of cement production by substituting a portion of ordinary Portland cement (OPC), while also enhancing material properties. A mixture of Portland cement and water is called cement paste. The chemical reactions between the components of Portland cement and water are known as cement hydration, which leads to the hardening of the paste, hence the term "hardened Portland cement paste" [1]. During hydration, new solid phases are chemically formed: one is crystalline calcium hydroxide, and the other—more commonly known—is "cement gel," which is amorphous [2, 3]. Fresh Portland cement paste consists of cement grains dissolved in water during mixing. In its hardened state, it is composed of solid reaction products and water-filled pores [4, 5]. The fresh paste is a network of suspended cement particles in water. It remains plastic for about an hour or more when it undergoes minor settling or "bleeding" [1]. The dried paste is highly porous, leading to the earlier belief that the physical structure of hardened paste was predominantly made up of pores [1].

Hardened cement paste exhibits a multiscale and multicomponent pore structure. The pores within the paste can be categorized into four types: air voids (larger than a few micrometers), small capillary pores (10–100 nm), large capillary pores (100–1000 nm), and gel pores (around 10 nm) [6, 7].

Cement paste is an inherently porous and permeable material due to its structural characteristics, comprising a dry solid matrix with randomly arranged particles. The overall porosity depends on factors such as the initial water content, the extent of space filled with hydration products, the water-cement (W/C) ratio, and curing conditions [8, 9]. The W/C ratio is especially significant in practical applications, yet the primary determinant of hardened cement paste properties is the quantity and size of pores. These include (i) gel pores (interlayer gaps in C–S–H), (ii) capillary pores, and (iii) air voids, each significantly impacting the paste's characteristics.

The gel pores are particularly small, approximately 2 nm in size, and contain around 28% gel water [10]. Due to their minimal size, these pores do not adversely affect the strength or permeability of the cement paste during hydration. When the mixture contains more water than needed for complete hydration, about 18.5% remains in the capillary pores as excess water [11–13]. With increased hydration, porosity decreases, leading to an improvement in paste strength, regardless of whether the capillary pores are water-filled [14].

In hydrated cement paste, water exists in two primary forms: (i) hydrate water, which integrates into the cement gel's pores as a structural component, and (ii) pore water. Pore water can be further classified as monolayer water (adsorbed on the gel surface), multilayer-adsorbed water, micropore water (condensed within pores smaller than 10^{-5} cm in radius), and macropore water [15, 16]. Additionally, interlayer water serves as a transitional link between the pore water and the hydrate structure, providing continuity between the hydrate water and pore water components [17, 18].

Cement paste undergoes a transition from a malleable state to a solid structure through the hydration process, a chemical reaction between cement and water [19, 20]. Various factors—including the type and application of admixtures, cement type, and curing conditions—can significantly influence the density and compressive strength of the resulting cement paste in concrete [21]. Curing, which promotes the cement's hydration process, involves managing both temperature and moisture transfer within the concrete structure [22]. Effective curing is crucial, as it enhances both the density and compressive strength of the concrete [21]. In a cement paste mixture, the volume occupied by hydration products increases as water content rises for a given proportion of cementitious materials. However, the hydration product volume remains constant at any specific hydration level, irrespective of water content. Consequently, the presence of unfilled pores, capillary spaces, and gel voids in the cement matrix leads to increased porosity and reduced density in concrete [15, 23].

During the early stages of mixing, a water film forms around the cement particles, leading to a higher water-to-cement ratio at the particle interface compared to the bulk paste. This condition facilitates the formation of larger calcium hydroxide and ettringite crystals, resulting in higher porosity and lower density within this interface region relative to the bulk cement paste [24, 25]. Over time, as hydration progresses, the formation of additional hydration products reduces both the volume and size of gel and capillary pores, leading to an improved microstructure [26].

Each year, global wheat production reaches around 790 million tonnes, highlighting wheat's importance as one of the most nutritionally valuable grains [27]. Wheat husk, a byproduct of this production, is primarily composed of carbon, oxygen, silica, and potassium, along with smaller quantities of sulfur, phosphorus, sodium, magnesium, and aluminum [28, 29].

When processed into ash, wheat husk consists of 85% to 90% amorphous silica, which can combine with calcium hydroxide to enhance material strength [30]. Given that cement manufacturing is a major source of greenhouse gas

emissions, including approximately 7% of global carbon dioxide emissions, incorporating rice straw and husk into concrete is both economically beneficial and environmentally friendly. Additionally, Portland cement production is associated with high costs, reinforcing the value of alternative materials like agricultural byproducts in concrete mixtures [31, 32].

Examined the effects of partially replacing cement with wheat husk ash (WHA) in a concrete design mix. Their analysis revealed that various industrial byproducts, such as fly ash, rice husk ash, ceramic and industrial waste, waste paper pulp, waste glass powder, marble dust, quarry dust, lime powder, and cow dung ash, can be used in different ratios to substitute portions of concrete components. Previous research included assessing the split tensile strength, flexural strength, and compressive strength of HCP at 7, 14, and 28 days. They concluded that when these materials are used in appropriate amounts, they can enhance concrete's strength, durability, and workability [33].

Similarly, demonstrated that substituting 20% of Portland cement with rice husk ash maximized compressive strength in concrete at 28 days. The study supports previous findings that cementitious materials incorporating rice husk ash yield higher compressive strengths than those without it. However, while rice husk ash improves early compressive strength, consensus on its long-term effects remains inconclusive [34].

While numerous studies have focused on the use of rice husk ash and fly ash in cementitious materials, limited research has been conducted on wheat husk ash (WHA). This study investigates its potential to enhance the mechanical and environmental properties of hardened cement paste (HCP), particularly at optimal replacement levels. Various proportions of WHA were incorporated into the cement mixture, and the resulting cement pastes were evaluated for compressive strength across different curing periods. Additionally, the influence of WHA on bulk density and water-to-cement ratio was assessed to provide a comprehensive understanding of its impact on HCP properties. The findings of this research could support the development of more sustainable and environmentally friendly cement-based materials through the use of agricultural byproducts, aligning with global efforts to reduce environmental pollution and industrial waste.

2 Materials and methods

2.1 Materials

The Portland cement grade (42.5 N) used in this study was produced by the Ziliten Cement Factory in Libya, in accordance with Libyan standard specifications No. 340/2009 [33]. The chemical, physical, and mechanical properties of this cement, as specified by the standard (340/2009), are presented in Tables 1 and 2, respectively. A sample of the Portland cement used in this research is shown in Fig. 1.

The water used in the present research experiments had a pH of 6.07, indicating a slightly acidic nature (pH < 7). The chemical composition of this water is provided in Table 3. Additionally, the physical and mechanical properties of the Portland cement (42.5 N, conforming to standard 340/2009) utilized in these experiments are listed in Table 2.

Table 1 Chemical standards of Portland cement (340/2009) 42.5 used in the present research experiments

Description	Maximum limit of permitted percentage
Insoluble reduce %	–
Sulfur third oxide	03.5
Magnesium oxide	05.0
Chlorides	00.1
Alkali content	–
Tricalcium silicate (C_3 S)	35.0
Dicalcium silicate (C_2 S)	40.0
Tricalcium aluminate (C_3 A)	7.00

Table 2 Physical and Mechanical Standards of Portland Cement (340/2009) 42.5 N used in the present research experiments

Description	Specification		
Compressive strength	Early strength		Standard strength
	2 days	7 days	28 days
	20 MPa	–	42.5–62.5 MPa
Initial setting time (min) not less than	60		
Soundness (distension)	Lochatellet not exceeding (mm)		Autoclave not exceeding (%)
	10		0.8
Heat hydration (joule/g) not exceeding	7 days		28 days
	250		290
Whiteness for white cement	80%		

Fig. 1 Portland cement used in the present research experiments

Table 3 Chemical content of water in mm/L used in the present research experiments

SO_4	Ca	Mg	Na	Cl	T. D. S
11.6	18.0	5.76	34.0	34.0	175.0

The wheat straw was thoroughly washed to remove dust and impurities, followed by air drying in an open environment. The dried wheat husk was burned at 600 °C for 2 h to maximize the yield of SiO_2 while ensuring the formation of an amorphous structure, and the ash was sieved using a 75-micron mesh for uniformity.

Figure 2 illustrates the processing stages: Fig. 2a shows a sample of wheat husk; Fig. 2b displays the washed wheat husk; Fig. 2c captures the air-drying process; Fig. 2d depicts the burning of the wheat husk; Fig. 2e presents the obtained WHA after burning. Additionally, Fig. 2f illustrates the screening device and a sample of the screened WHA, respectively, while Fig. 2g shows the WHA being weighed using an electronic balance.

For the present experiments, a cube frame for HCP samples was utilized. This wooden geometric structure was divided into 30 cubes, each with dimensions of 3.5 cm × 3.5 cm × 3.5 cm for length, width, and depth, as shown in Fig. 3.

2.2 Estimation of WHA parameters

2.2.1 Estimation of internal density and apparent porosity

The internal density of hardened cement paste (HCP) denotes the compactness and arrangement of solid components inside its microstructure, which greatly influences its mechanical properties and endurance. An increased internal density signifies superior particle packing, less porosity, and improved cohesion among cementitious phases, including calcium silicate hydrate (C–S–H) gel and calcium hydroxide. This results in enhanced compressive strength and reduced permeability, hence increasing the material's resistance to environmental deterioration. Conversely, reduced internal

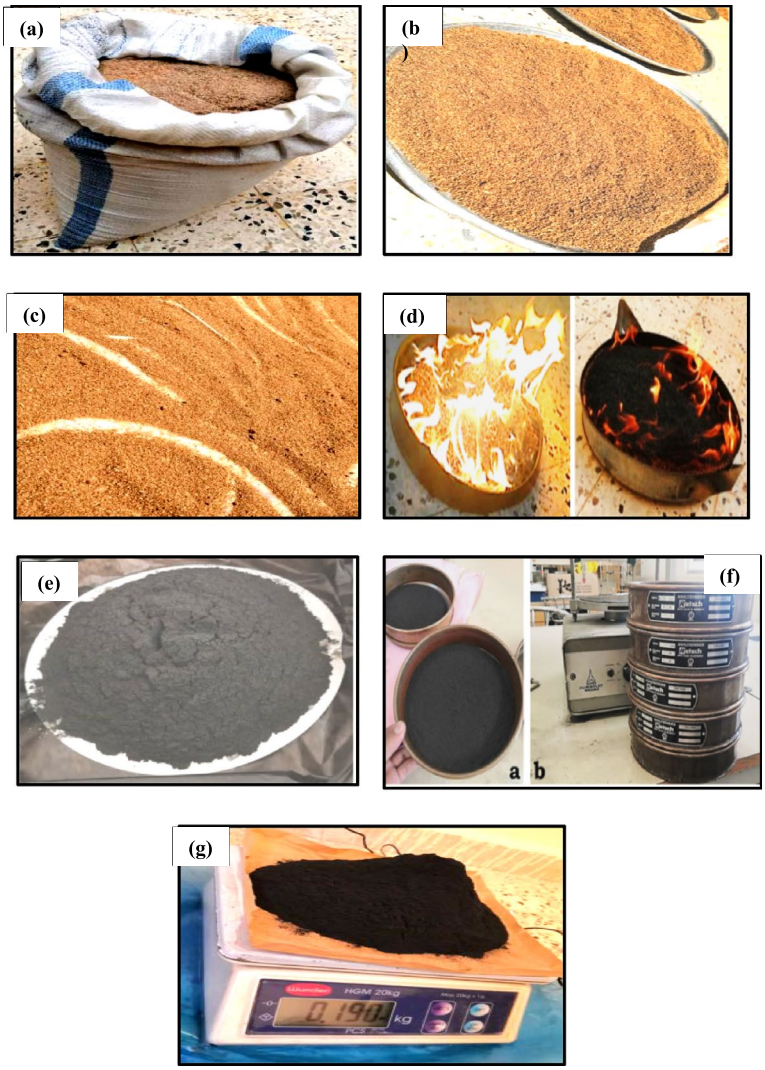

Fig. 2 Processing stages of wheat husk ash (WHA) production

Fig. 3 Frame mold for HCP samples

density indicates heightened porosity, potentially compromising structural integrity and diminishing long-term durability. The integration of wheat husk ash (WHA) in HCP has been shown to affect internal density by optimizing pore structure

and augmenting particle interaction, hence promoting sustainability and boosting performance in building applications [34, 35].

(i) For each ratio of WHA (0%, 5%, 10%, 15%, 20%, 25%, and 30%), two HCP samples (balls) were prepared. The samples were dried at 110 °C for 1 h, then removed from the oven, and their dry weight ($\mathbf{W_{dry}}$) was recorded. (ii) The dried samples of all proportions were immersed in water, heated on a heating plate for about 1 h until the water reached evaporation, and subsequently weighed. These samples were classified as saturated, with their weight recorded as ($\mathbf{W_{sat.}}$). (iii) Each ball was attached to a copper thread and suspended in a half-filled cup of water placed on a balance. The weight of the suspended sample ($\mathbf{W_{susp.}}$) was recorded after zeroing out the initial weight of the cup. The standard test method: Chemically combined water, Bulk density, Apparent porosity, compressive strength.

The following formulas were used to compute the apparent porosity and bulk density:

$$B.D = \frac{W_{dry}}{W_{sat.} - W_{susp.}} * \rho \tag{1}$$

$$\%A.P = \frac{W_{sat.} - W_{dry}}{W_{sat.} - W_{susp.}} * 100 \tag{2}$$

2.2.2 Chemically combined water examination

Chemically mixed water denotes the water that is an essential component of the hydration products of cement, namely in the development of C–S–H gel, calcium hydroxide, and other hydrated compounds. In contrast to loose water, which either resides in the pores or evaporates over time, chemically coupled water is integrally linked inside the cement matrix [36].

The quantification of chemically combined water is essential in this work, as it elucidates the level of cement hydration, the magnitude of pozzolanic reactions when supplemental cementitious materials such as wheat husk ash (WHA) are included, and the overall durability of the hardened cement paste. Comprehending chemically mixed water aids in evaluating the material's long-term stability, strength progression, and resistance to deterioration. This research seeks to assess the effectiveness of WHA as a partial substitute for cement by analyzing the chemically mixed water content, with the goal of boosting the hydration process and improving the microstructural integrity of cementitious materials.

All samples were ground using a solid cement mortar and dissolved in an equal mixture of ether and methyl alcohol at a 1:1 ratio. The mixture was then placed in a drying oven at 110 °C for 1 h. Afterward, the samples were removed from the oven, and each was weighed, with the weight recorded as ($\mathbf{W_{before\ burning}}$).

Subsequently, each sample was heated on a heating plate at approximately 800 °C for an additional hour. The final weight of each sample was measured and recorded as ($\mathbf{W_{after\ burning}}$).

The proportion of chemically combined water for each **WHA** HCP ball was determined using the following equation:

$$\%C.C.W = \frac{W_{before\ burning} - W_{after\ burning}}{W_{before\ burning}} \times 100 \tag{3}$$

2.3 Experimental program

In the experimental program, a segment of Portland cement in the mixture was substituted with varied percentages of WHA% to assess the compressive strength of HCP. Prior to use WHA as a supplemental cementitious material, it is essential to ascertain its basic oxide composition and pozzolanicity to confirm its pozzolanic properties. Wheat husk ash (WHA) is acknowledged for its substantial silica (SiO_2) concentration, making it a viable pozzolanic material for cementitious applications. The chemical composition of WHA may vary depending on the combustion method and circumstances. Nevertheless, literature reveals the following typical properties of oxide composition:

Silicon Dioxide (SiO_2): WHA mostly consists of silica. A research indicated that WHA has around 92.3% SiO_2, which elevated to 99.3% after acid leaching [37].

A separate investigation identified a silica concentration of 43.22% in WHA produced at 600 °C. Furthermore, studies revealed a silica concentration of 56% in WHA. These differences underscore the impact of processing conditions on silica content.

The alumina concentration in WHA differs across research. One research indicated an alumina concentration of 21%, however another investigation found no detectable Al_2O_3 in WHA. This mismatch indicates that variables like the origin of the wheat husk and the processing techniques may substantially affect the alumina content. The calcium oxide (CaO) concentration in WHA exhibits variability. One research indicated a CaO level of 12.2%, whereas another investigation revealed a reduced CaO content of 0.29%. These discrepancies may arise from changes in the origin of the wheat husk and the combustion process. The magnesium oxide (MgO) concentration in WHA is generally minimal. A research indicated a MgO level of 0.5%, whilst another investigation revealed a MgO value of 0.34%. The concentration of Ferric Oxide (Fe_2O_3) in WHA differs throughout several investigations. One research indicated a Fe_2O_3 concentration of 6.5%, whereas another investigation revealed a Fe_2O_3 concentration of 0.29% [38].

These variations in oxide composition underscore the importance of characterizing WHA from specific sources before its application in cementitious materials. In this study, Portland cement was partially replaced with WHA at 0, 5, 10, 15, 20, 25, and 30%. Samples were mixed for 5 min, cast into molds, and cured in water at 27 °C for 3, 7, 14, and 28 days. A total of 56 samples were prepared and tested during the study. Table 4 presents the substitution details for Portland cement with WHA%.

The mix proportions were carefully controlled to ensure uniformity and reproducibility across all samples. The procedure involved:

Weighing of materials: Precise weights of Portland cement and WHA were measured according to the replacement percentages (e.g., 0%, 5%, 10%, 15%, 20%, 25%, and 30%).

Mixing process: The dry components (cement and WHA) were thoroughly mixed for 2 min to ensure homogeneity. Subsequently, water was added to the dry mix at a water-to-cement ratio of 0.5, and mixing continued for an additional 3 min using a mechanical mixer.

Casting and curing: The resulting paste was immediately cast into molds, compacted to minimize air voids, and cured in water at 27 °C for the designated durations (3, 7, 14, and 28 days).

This controlled methodology ensured consistency and reliability in sample preparation, enabling a meaningful comparison of results across different WHA replacement levels.

Figure 4a and b show the schematic diagrams cubes and balls of HCP, respectively, used in the experiments of the current research. The cubes were removed from the frame molds after 24 h. Both the HCP balls and cubes were numbered for identification before being submerged in fresh water (27 °C ± 3). The immersion durations were 3, 7, 14, and 28 days. The standard test method: chemically combined water, bulk density, apparent porosity, compressive strength.

Prior to the compressive strength test, each sample was ground and polished to create a smooth and flat surface, minimizing errors when reading the loading force during the test. A compressive strength testing machine with a capacity of 2000 kN was used to perform the test on the HCP cube samples. The applied stress was delivered at a rate of approximately 140 kg cm^{-2} min^{-1}.

Table 4 Prepared samples with Portland cement replaced by WHA%

Sample No	Portland cement (wt. %)	(WHA) (wt. %)
1	100	00
2	95	05
3	90	10
4	85	15
5	80	20
6	75	25
7	70	30

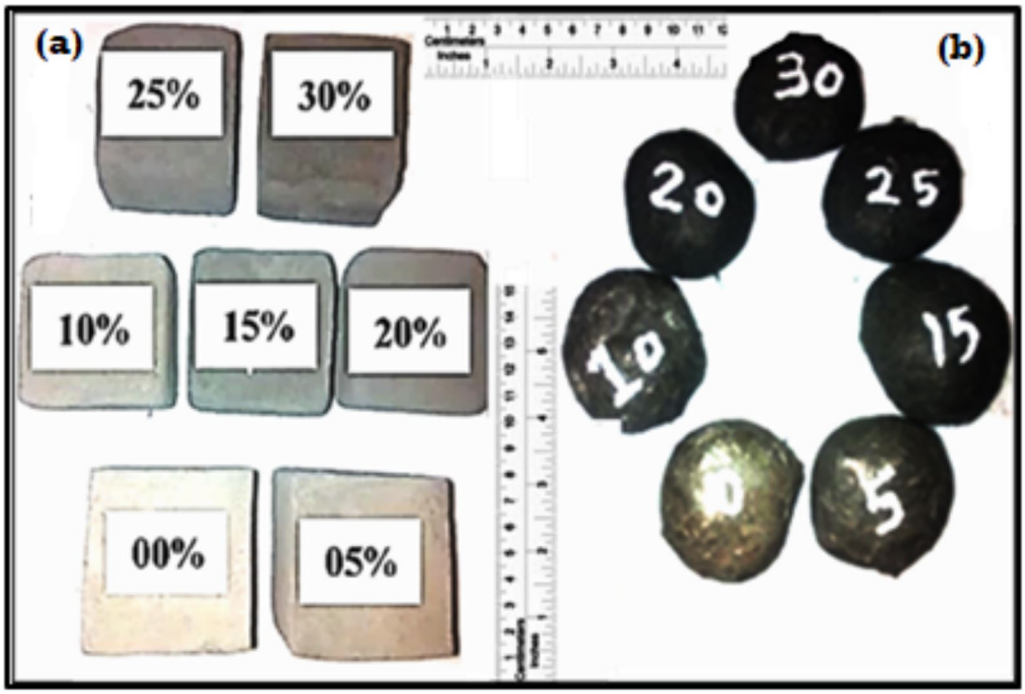

Fig. 4 The cubes and balls of HCP, respectively, used in the experiments of the current research

3 Results and discussion

According to the results, it was found that the water requirement for a sample of HCP at standard consistency increased linearly as WHA% increased. This can be attributed to the hygroscopic nature of WHA, which absorbs proportionally higher amounts of mixing water, a finding consistent with observations made in other studies [39, 40]

The connection between water consistency and WHA% in HCP is depicted in Fig. 5. The findings indicated that the total water content progressively increased with higher levels of WHA%. The highest water consistency of HCP was recorded at 15% WHA by weight. However, as the WHA% rose to 20%, 25%, and 30%, the water consistency in HCP gradually declined.

Figure 6 shows the chemically combined water content of HCP samples at different curing ages.

Figure 7 illustrates the effect of WHA (%) on the bulk density of HCP mixes at different curing times. At 3 days of curing, the bulk density of HCP decreases gradually as the WHA percentage increases from 0 to 30%, with values dropping from 2450 to 1830 kg/m^3.

A similar trend is observed at 7 days of curing, where the bulk density decreases from 2500 to 1810 kg/m^3. After 14 days of curing, the bulk density continues to decrease, ranging from 2600 to 1800 kg/m^3 as WHA (%) increases. By 28 days of curing, the maximum bulk density (2880 kg/m^3) is observed at 0% WHA, but with increasing WHA percentages, the

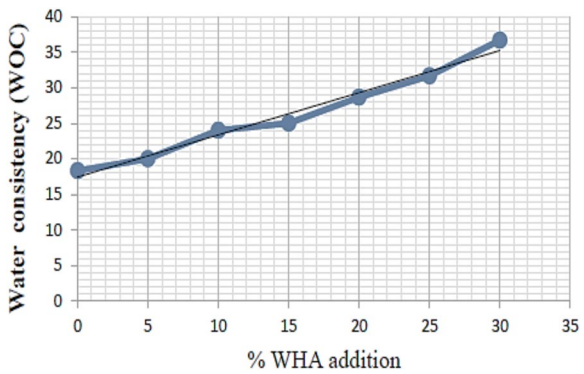

Fig. 5 Water consistency of different cement mixes

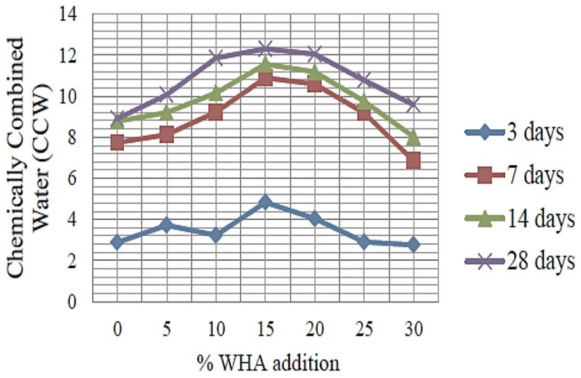

Fig. 6 Chemically combined water of different (HCP) samples

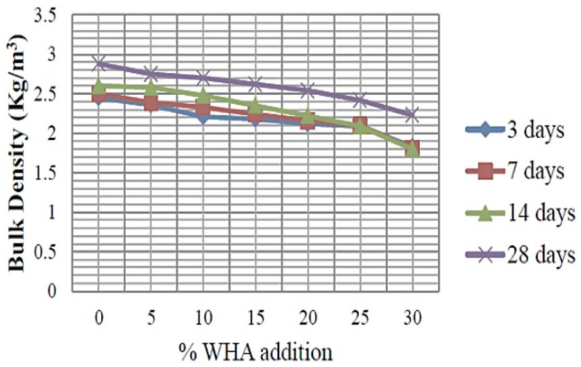

Fig. 7 Bulk density of HCP mixes containing varying percentages of WHA (%) at different curing times

bulk density decreases to 2230 kg/m^3. At 0% WHA, the concrete contains traditional dense materials like cement and aggregates, leading to a higher bulk density (2880 kg/m^3). As the percentage of WHA increases, these dense materials are progressively replaced, leading to a lighter, less dense mix, WHA can increase the porosity of the concrete. This occurs because WHA particles are typically finer and less dense, leading to a less compact matrix. More voids in the structure result in a lower bulk density. In summary, the maximum bulk density is observed at 0% WHA because the mix is fully composed of dense materials. As WHA percentages increase, the lighter and more porous nature of WHA reduces the bulk density to 2230 kg/m^3.

Overall, the bulk density of HCP samples increases with longer curing times due to the formation of hydration products that fill some of the pore volume. This densification enhances the structural compactness of the HCP matrix over time [41]. The increase in bulk density with longer curing times is observed under standard curing conditions (immersion in water at 27 °C). These conditions promote continuous hydration of cementitious materials, allowing the formation of hydration products such as calcium silicate hydrates (C–S–H) and calcium hydroxide (CH).

As curing progresses, these hydration products gradually fill the available pore spaces in the HCP matrix, reducing voids and increasing the matrix's overall density. This densification process is more pronounced at early curing stages (e.g., up to 14 days), as hydration activity is at its peak during this period. After 14 days, the rate of hydration slows down, resulting in a smaller incremental increase in bulk density.

Figure 8 highlights the effect of WHA (%) on the apparent porosity of HCP mixes over varying curing times. At 3 days of curing, the apparent porosity increases from 15.03 to 22.82% as WHA percentage rises from 0 to 30%. This trend continues at 7 days of curing, where apparent porosity increases from 9.86% to 20.36%. After 14 days of curing, the apparent porosity further rises from 7.16 to 18.34%, and by 28 days of curing, it increases from 6.23 to 18.11% with increasing WHA percentages. The trend of declining porosity in hydrated cement paste (HCP) samples with extended curing times can be explained by the hydration process of cement with water, chemical reactions occur, primarily forming calcium silicate hydrate (C–S–H) and calcium hydroxide (CH). These products contribute to the strength and density of the HCP, Initially, freshly mixed HCP contains a significant amount of water and unhydrated cement particles, leading to high porosity. Over time, the hydration reaction continues, and the hydration products gradually fill the pore spaces within the matrix.

Apparent porosity also shows a general decreasing trend with extended curing times, reflecting the densification of the HCP matrix. For instance, at 0% WHA, apparent porosity decreases significantly from 15.03% at 3 days to 6.23% at 28 days, representing a reduction of approximately 60%. A similar decrease is observed at 5% WHA, where

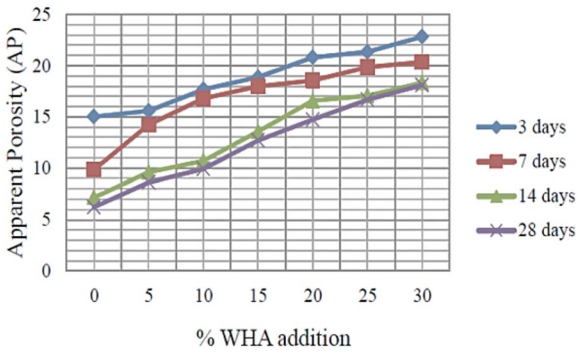

Fig. 8 Apparent porosity of HCP mixes containing varying percentages of WHA (%) at different curing times

apparent porosity drops from 15.58 to 8.63% over the same curing period, marking a 45% reduction. At 10% WHA, the apparent porosity decreases from 17.68 to 9.93% (44% reduction), while at 15% WHA, it decreases from 18.87 to 12.71% (33% reduction).

For 20% WHA, apparent porosity decreases from 20.81 to 14.73% over 3–7 days but shows a slight increase to 16.58% at 14 days before decreasing again to 14.73% by 28 days. At 25% WHA, the apparent porosity decreases from 21.34 to 16.69% over 3–7 days, increases to 30.06% at 14 days, then decreases again to 16.69% by 28 days. Similarly, at 30% WHA, apparent porosity decreases from 22.82 to 18.11% over 3–7 days, increases to 18.34% at 14 days, and decreases again to 18.11% at 28 days.

Porosity plays a crucial role in determining the material's properties, particularly its strength. High porosity typically results in lower material strength, while reduced porosity enhances compressive strength. This inverse relationship between porosity and compressive strength is well-documented, demonstrating that materials with lower porosity exhibit improved structural performance [42, 43]. In essence, this trend demonstrates that the porosity of HCP decreases over time because the ongoing hydration process progressively occupies available pore spaces with solid hydration products, densifying the material.

The results presented in Fig. 8 indicate that the total porosity of all HCP samples containing varying WHA% decreased progressively with longer curing durations. At a curing time of 3 days, all samples exhibited higher porosity levels, while the lowest total porosity was observed at 28 days of curing. This trend suggests that the porosity of HCP samples declines with extended curing times due to the ongoing hydration process, during which hydration products gradually occupy available pore spaces. The decline in porosity with extended curing times is directly related to the progression of the cement hydration process. During hydration, Portland cement reacts with water to produce compounds such as calcium silicate hydrates (C–S–H) and calcium hydroxide (CH). These hydration products are solid and progressively fill the pore spaces in the cement matrix, thereby reducing the total volume of pores.

This trend is particularly evident in the early curing stages (up to 14 days), where hydration activity is vigorous. As curing time extends beyond 14 days, the reduction in porosity becomes less pronounced due to the diminishing availability of unhydrated cement particles. The observed trend is consistent with established studies on the hydration and densification of cementitious materials, confirming the effectiveness of proper curing in enhancing structural compactness.

When plain concrete is subjected to compression, failure typically occurs along the diagonal plane of the vertical member. This failure results from lateral tensile forces causing vertical cracks. Under an axial compressive load, microcracks form along the vertical axis of the concrete member and subsequently propagate due to lateral tensile strains.

The compressive strength of the HCP samples was determined using the following formula:

$$\sigma_c = \frac{F_L}{A} \tag{4}$$

where F_L represents the failure load recorded by the testing machine at the point of concrete failure and (A) represents the sample's cross-sectional area. The dimensions of the HCP cube samples were (3.5 cm × 3.5 cm × 3.5 cm), representing the length, width, and height, respectively. Using Eq. (4), the cross-sectional area (A) was calculated as:

$$A = 3.5 \times 3.5 = 12.25\ cm^2 = 1.225 \times 10^{-3}\ m^2.$$

Table 5 Compressive strength results of HCP samples containing different WHA% after 28 days of curing

Sample no	(WHA) (%)	Failure load average (kN)	Compressive strength (Mpa)	Compressive strength decreasing (%)
Blank	–	31.70	25.88	0.00
H1	05.00	30.40	24.82	−04.1
H2	10.00	28.60	23.35	−09.8
H3	15.00	36.80	30.04	+13.8
H4	20.00	35.20	28.73	+09.9
H5	25.00	21.40	17.47	−32.5
H6	30.00	12.70	10.37	−59.9

Table 5 summarizes the compressive strength results for HCP cube samples at various WHA% after 28 days of curing. Before conducting the compression strength tests, HCP cube and ball samples were cured in clean, fresh water devoid of any contaminants for 3, 7, 14, and 28 days. This curing process prevented water evaporation from the cement paste, ensuring optimal hydration.

Table 5 and Fig. 9 illustrates the relationship between the percentage of WHA in HCP and the corresponding compressive strength. Based on the failure load results of the HCP samples, the compressive strength was calculated using Eq. (4), with the results listed in Table 5. The analysis revealed the following trends: for 5.00% WHA, the compressive strength decreased from 25.88 MPa (control) to 24.82 MPa, representing a 4.00% reduction compared to the non-incorporated HCP sample. With 10.00% WHA, the compressive strength dropped further to 23.35 MPa, a reduction of 10.00%. Interestingly, at 15.00% WHA, the compressive strength increased to 30.04 MPa, an enhancement of 14.00%. When WHA was increased to 20.00%, the compressive strength slightly declined to 28.73 MPa, but this still marked a 10.00% improvement compared to the control. However, with 25.00% WHA, the compressive strength dropped sharply to 17.47 MPa, indicating a significant 33.00% reduction. Finally, at 30.00% WHA, the compressive strength fell drastically to 10.37 MPa, a 60.00% reduction from the control sample. The observed increase in compressive strength at 15% WHA is attributed to the pozzolanic reaction between the amorphous silica in WHA and the calcium hydroxide produced during hydration. Similar trends have been reported in studies using rice husk ash. However, beyond 15% replacement, the strength decreases due to increased porosity and reduced matrix densification.

These results indicate that the maximum enhancement in compressive strength occurred at 15.00% WHA, with a 14.00% improvement, followed by a 10.00% enhancement at 20.00% WHA. Conversely, WHA levels of 5.00%, 10.00%, 25.00%, and 30.00% resulted in reduced compressive strengths, with the most pronounced decline of 60.00% observed at 30.00% WHA.

Overall, the findings demonstrate that porosity decreases with curing age across all HCP samples. The samples containing 15.00% and 20.00% WHA exhibited superior early-age strength development, likely due to improved hydration reactions compared to those with lower (5.00% and 10.00%) or higher (25.00% and 30.00%) WHA content. Samples with 15.00% WHA achieved the best performance, producing comparable or superior strength relative to the control.

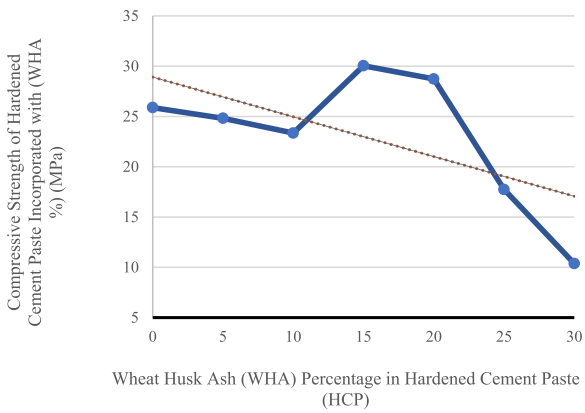

Fig. 9 Relationship between WHA percentage and the compressive strength of HCP samples at 28 days curing time

These results align with previous research, which highlights the use of fly ash in cement production and its impact on strength development [44, 45]. Specifically, the fineness and granulometry of fly ash significantly influence mortar strength, as finer particles accelerate hydration reactions by acting as nucleation sites [46, 47].

4 Conclusion

This study investigated the effects of chemically combined water, bulk density, porosity, and compressive strength in hardened cement paste (HCP) samples with varying levels of wheat husk ash (WHA). The results revealed that chemically combined water increased with higher WHA percentages, peaking at 15 wt.% and showing significant growth as the curing age progressed from 3 to 14 days. Beyond this period, the increase became minimal as the hydration process approached completion.

Bulk density decreased with increasing WHA content, which is attributed to the lower density of WHA. Conversely, apparent porosity increased with greater WHA incorporation due to the higher porosity of the WHA particles. Compressive strength improved significantly with WHA content up to 15 wt.%, outperforming the control samples. At 20 wt.% WHA, compressive strength showed a slight decline but remained comparable to the control. However, WHA levels exceeding 20 wt.% (e.g., 25–30 wt.%) resulted in a notable reduction in compressive strength.

This study concludes that incorporating WHA in HCP can enhance compressive strength at optimal levels, particularly at 15 wt.%, where a balance between strength and material efficiency is achieved. The findings of this study highlight the potential of wheat husk ash (WHA) as a sustain-able cement replacement material. With optimal WHA incorporation (15–20%), the mechanical properties, including compressive strength and density, showed significant improvements. These results suggest that WHA-blended cement could be suitable for structural applications, particularly in eco-friendly construction projects. Further research is recommended to evaluate its performance in reinforced concrete structures and the future research should focus on evaluating the long-term durability and performance of WHA-based materials in real-world applications, including their resistance to environmental factors and compatibility with other cementitious additives.

Author contributions M.F. Conceptualization, data curation, and drafting of the manuscript. M.A.A. Methodology development, data analysis, and validation. T.A. Conducted experiments, reviewed, and contributed to manuscript preparation. M.E. Assisted in experimental design, results interpretation, and manuscript editing. A.S. Provided resources, data acquisition, and manuscript review. A.S. provided resources, data acquisition, and Contributed to experimental analysis. F.F. Contributed to experimental analysis, manuscript editing, and technical support. Y.K. Supervision of research work, funding acquisition, and final manuscript review.

Funding No Funding.

Data availability The datasets generated during and/or analysed during the current study are available from the corresponding author on reasonable request.

Declarations

Ethics approval and consent to participate Not applicable.

Consent for publication Not applicable.

Competing interests The authors declare no competing interests.

Open Access This article is licensed under a Creative Commons Attribution-NonCommercial-NoDerivatives 4.0 International License, which permits any non-commercial use, sharing, distribution and reproduction in any medium or format, as long as you give appropriate credit to the original author(s) and the source, provide a link to the Creative Commons licence, and indicate if you modified the licensed material. You do not have permission under this licence to share adapted material derived from this article or parts of it. The images or other third party material in this article are included in the article's Creative Commons licence, unless indicated otherwise in a credit line to the material. If material is not included in the article's Creative Commons licence and your intended use is not permitted by statutory regulation or exceeds the permitted use, you will need to obtain permission directly from the copyright holder. To view a copy of this licence, visit http://creativecommons.org/licenses/by-nc-nd/4.0/.

References

1. Powers TC. Structure and physical properties of hardened Portland cement paste. J Am Ceram Soc. 1958;41:1–6.
2. Pickett G. Shrinkage stresses in concrete. In: J. Proc.; 1946. p. 165–204.
3. Hou D. Molecular simulation on cement-based materials. Springer; 2020.
4. Sutter LL. Materials-related distress: hardened cement paste best practices for jointed concrete pavements. Federal Highway Administration; 2015.
5. Lavagna L, Nisticò R. An insight into the chemistry of cement—a review. Appl Sci. 2022;13:203.
6. Babaei S. A multiscale approach to model thermo-hydro-mechanical behaviour of nonreinforced concrete; 2021.
7. Yio MHN, Wong HS, Buenfeld NR. 3D pore structure and mass transport properties of blended cementitious materials. Cem Concr Res. 2019;117:23–37.
8. Mamun M. The fractal nature of cement-based systems under sustained elevated temperatures; 2018.
9. Tracz T, Zdeb T. Effect of hydration and carbonation progress on the porosity and permeability of cement pastes. Materials (Basel). 2019;12:192.
10. Pansuk W. Properties of hardened concrete, vol. 2. New York: Pergamon Press; 2011. p. 24.
11. Schoeman M. Investigating the relationship between suction in cement paste and specific concrete properties; 2020.
12. Ramezanianpour AA. Cement replacement materials. Geochem Mineral. 2014;10:973–8.
13. Georget F, Sui S, Wilson W, Scrivener KL. Reconciliation of pore structure characterization methods: the simple case of PC-limestone cement pastes. Cem Concr Res. 2024;184: 107624.
14. Šavija B, Luković M. Carbonation of cement paste: understanding, challenges, and opportunities. Constr Build Mater. 2016;117:285–301.
15. Jennings HM, Bullard JW, Thomas JJ, Andrade JE, Chen JJ, Scherer GW. Characterization and modeling of pores and surfaces in cement paste: correlations to processing and properties. J Adv Concr Technol. 2008;6:5–29.
16. Zeng Q, Zhang D, Sun H, Li K. Characterizing pore structure of cement blend pastes using water vapor sorption analysis. Mater Charact. 2014;95:72–84.
17. Fang Z, Wang C, Hu H, Zhou S, Luo Y. Effect of electrical field on the stability of hydration products of cement paste in different liquid media. Constr Build Mater. 2022;359: 129489.
18. Hou D, Zhao T, Ma H, Li Z. Reactive molecular simulation on water confined in the nanopores of the calcium silicate hydrate gel: structure, reactivity, and mechanical properties. J Phys Chem C. 2015;119:1346–58.
19. Pichler B, Hellmich C. Upscaling quasi-brittle strength of cement paste and mortar: a multi-scale engineering mechanics model. Cem Concr Res. 2011;41:467–76.
20. Kawashima S, Chaouche M, Corr DJ, Shah SP. Influence of purified attapulgite clays on the adhesive properties of cement pastes as measured by the tack test. Cem Concr Compos. 2014;48:35–41.
21. Falliano D, De Domenico D, Ricciardi G, Gugliandolo E. Experimental investigation on the compressive strength of foamed concrete: effect of curing conditions, cement type, foaming agent and dry density. Constr Build Mater. 2018;165:735–49.
22. Nie S, Hu S, Wang F, Yuan P, Zhu Y, Ye J, Liu Y. Internal curing–a suitable method for improving the performance of heat-cured concrete. Constr Build Mater. 2016;122:294–301.
23. Hlobil M, Kumpová I, Hlobilová A. Surface area and size distribution of cement particles in hydrating paste as indicators for the conceptualization of a cement paste representative volume element. Cem Concr Compos. 2022;134: 104798.
24. Milenković N. Contribution to the development of an additive for bulk waterproofing of cement-based materials; 2017.
25. Ehsani A. Effects of power ultrasound on the pore solution, hydration and mechanical properties of Portland cement pastes and mortars; 2021.
26. Ge W, Zhang Z, Ashour A, Li W, Jiang H, Hu Y, Shuai H, Sun C, Li S, Liu Y. Hydration characteristics, hydration products and microstructure of reactive powder concrete. J Build Eng. 2023;69: 106306.
27. Holman JD, Obour AK, O'Brien D, Assefa Y. Historic winter wheat yield, production, and economic value trends in Kansas, the "Wheat State." Crop Sci. 2024;64:925–41.
28. Dodson J. Wheat straw ash and its use as a silica source; 2011.
29. Steven S, Restiawaty E, Bindar Y. Routes for energy and bio-silica production from rice husk: a comprehensive review and emerging prospect. Renew Sustain Energy Rev. 2021;149: 111329.
30. Amran M, Fediuk R, Murali G, Vatin N, Karelina M, Ozbakkaloglu T, Krishna RS, Sahoo AK, Das SK, Mishra J. Rice husk ash-based concrete composites: a critical review of their properties and applications. Crystals. 2021;11:168.
31. Paris JM, Roessler JG, Ferraro CC, DeFord HD, Townsend TG. A review of waste products utilized as supplements to Portland cement in concrete. J Clean Prod. 2016;121:1–18.
32. Thomas BS, Yang J, Mo KH, Abdalla JA, Hawileh RA, Ariyachandra E. Biomass ashes from agricultural wastes as supplementary cementitious materials or aggregate replacement in cement/geopolymer concrete: a comprehensive review. J Build Eng. 2021;40: 102332.
33. Khalil NM, Hassan EM, Shakdofa MME, Farahat M. Beneficiation of the huge waste quantities of barley and rice husks as well as coal fly ashes as additives for Portland cement. J Ind Eng Chem. 2014;20:2998–3008.
34. Zhang L, Zhou J. Fractal characteristics of pore structure of hardened cement paste prepared by pressurized compact molding. Constr Build Mater. 2020;259: 119856.
35. Zhang H, Xu Y, Gan Y, Chang Z, Schlangen E, Šavija B. Microstructure informed micromechanical modelling of hydrated cement paste: techniques and challenges. Constr Build Mater. 2020;251: 118983.
36. John E, Lothenbach B. Cement hydration mechanisms through time–a review. J Mater Sci. 2023;58:9805–33.
37. Terzioğlu P, Yücel S, Öztürk M. Synthesis of zeolite NaA from a new biosilica source. Waste Biomass Valor. 2016;7:1271–7.
38. Terzioğlu P, Yücel S. Synthesis of magnesium silicate from wheat husk ash: effects of parameters on structural and surface properties. BioResources. 2012. https://doi.org/10.15376/biores.7.4.5435-5447.

39. Metha PK. The chemistry and technology of cement made from rice husk ash, UNIDO/ESCAPE CTT. In: Proceeding work. Rice husk ash cement; 1979.
40. Rukzon S, Chindaprasirt P. Strength of ternary blended cement mortar containing portland cement rice husk ash fly ash. Eng J Res Dev. 2006;17:33–8.
41. Li Y, Han D, Wang H, Lyu H, Zou D. Carbonation curing of mortars produced with reactivated cementitious materials for CO2 sequestration. J Clean Prod. 2023;383: 135501.
42. Forquin P, Arias A, Zaera R. Role of porosity in controlling the mechanical and impact behaviours of cement-based materials. Int J Impact Eng. 2008;35:133–46.
43. Hou D, Li D, Hua P, Jiang J, Zhang G. Statistical modelling of compressive strength controlled by porosity and pore size distribution for cementitious materials. Cem Concr Compos. 2019;96:11–20.
44. Das A. Strength characterisation fly ash composite material; 2009.
45. Zheng C, Liu Z, Xu J, Li X, Yao Y. Compressive strength and microstructure of activated carbon-fly ash cement composites. Chem Eng Trans. 2017;59:475–80.
46. Moghaddam F, Sirivivatnanon V, Vessalas K. The effect of fly ash fineness on heat of hydration, microstructure, flow and compressive strength of blended cement pastes. Case Stud Constr Mater. 2019;10: e00218.
47. Seifan M, Mendoza S, Berenjian A. A comparative study on the influence of nano and micro particles on the workability and mechanical properties of mortar supplemented with fly ash. Buildings. 2021;11:60.

Publisher's Note Springer Nature remains neutral with regard to jurisdictional claims in published maps and institutional affiliations.